A new approach to relativistic multi-configuration quantum mechanics in titanium

J.A. Lowe [a], C.T. Chantler [a,*], I.P. Grant [b]

[a] *School of Physics, University of Melbourne, Australia*
[b] *Mathematical Institute, Oxford University, Oxford, UK*

A R T I C L E   I N F O

A B S T R A C T

Multiply-ionized atoms in plasmas and astronomical systems are predominantly of intermediate atomic numbers with open electron shells. The spectra seen in laboratory plasmas and astrophysical plasmas are dominated by characteristic $K\alpha_{1,2}$ photoemission lines. Modelling these transitions requires advanced relativistic frameworks to begin to formulate solutions. We present a new approach to relativistic multi-configuration determination of $K\alpha_{1,2}$ diagram and satellite energies in titanium to a high level of convergence, allowing accurate fitting of satellite contributions and the first agreement with profile to negligible residuals. These developments also apply to exciting frontiers including temporal variation of fundamental constants, theoretical chemistry and laboratory astrophysics.

© 2010 Elsevier B.V. All rights reserved.

The need of astrophysics for tools with which to investigate plasmas has developed the field of laboratory astrophysics, in part to address questions like the variation of fundamental constants such as α and c with time [1]. Likewise, atomic calculations are necessary for complex plasma physics modelling, which is crucial in fusion development, and in potential diagnostics of reactor design [2]. In these areas — as in fundamental atomic physics, X-ray sources and condensed matter applications — the primary source of information and insight is that due to characteristic radiation, much of which arises from inner shell processes of open shell systems as exemplified by transition metals such as iron [3]. However, open shell systems are particularly difficult to model, requiring advanced relativistic theory to even begin the problem. This Letter addresses solutions to the problems posed by these difficult systems and demonstrates that new approaches to theory are now shedding light on our laboratories and on the universe.

Numerous approaches have been used to calculate atomic data, including Dirac–Fock combined with many-body perturbation theory (MBPT) [4], energy dependent MBPT [5], relativistic configuration interaction (RCI) [6], and multi-configuration Dirac Fock (MCDF). The MCDF method has been highly successful in simple atoms and valence shells since the sixties and seventies [7]. Different approaches have used alternate basis sets to orthogonalize key symmetries or for computational efficiency, as illustrated in Fig. 1. Nevertheless, inner-shell and multiple-open shell systems are far more challenging for existing methods to deal with due to issues including rapid growth of computation time, fail-

ure of convergence and multiple near-degenerate eigenstates. The MCDF method, based on the variational principle, is intrinsically difficult to manage for highly excited states. The $K\alpha$ transition $(1s^{-1} \rightarrow 2p^{-1})$ in the transition metals is a classic example of one such problem. The $K\alpha$ spectrum itself is used widely in astrophysics [8], plasma physics [9] and for chemical state characterization [10].

The structure of the $K\alpha$ profile in the transition elements has been the subject of many theoretical and experimental studies [11–13]. These studies were motivated by its asymmetric shape, indicative that processes are occurring other than the bound-bound transition from which the transition takes its label. Several mechanisms have been suggested for this asymmetry, including collective excitations from the conduction band [14], final state interactions [11] and shake processes [15]. It now appears that shake-off processes, which generate species with one or more extra holes that are passive when the 1s hole de-excites, are the major contributor to the structure observed and hence that the solid-state spectra may be dominated by atomic considerations [16].

Our work on titanium presented here is based on the MCDF method, which is described widely [17]. Atomic states are expanded into linear combinations of configuration state functions (CSFs) of well defined parity and angular momentum,

$$\Psi(\Pi J M) = \sum_r c_r \Phi(\gamma_r \Pi J M) \tag{1}$$

where $\Phi(\gamma_r \Pi J M)$ are linear combinations of Slater determinants, built from orthonormal Dirac spinors, having parity and angular momentum quantum numbers $\Pi J M$ forming an orthonormal basis, and γ_r contains all the quantum numbers necessary to dis-

* Corresponding author. Tel.: +61 3 8344 5437.
 E-mail address: chantler@unimelb.edu.au (C.T. Chantler).

$$R_{\lambda_p} \propto r^n e^{\Gamma \lambda_p r}$$

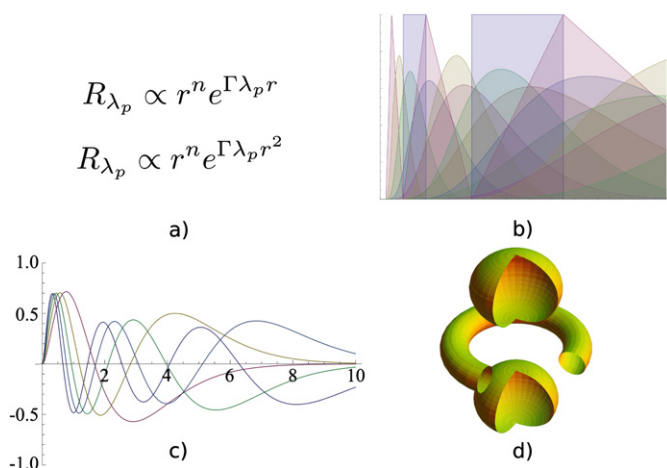$$R_{\lambda_p} \propto r^n e^{\Gamma \lambda_p r^2}$$

a)

b)

c)

d)

Fig. 1. Basis sets used in atomic structure algorithms. (a) Slater-type and Gaussian-type functions are common in quantum chemistry and are often computationally efficient. (b) Recursively generated B-splines are spatially localized functions, and have been successful in non-relativistic systems and in some relativistic codes. (c) Convergent-close-coupling uses damped oscillatory radial functions and has been applied to many scattering problems for few-electron systems. (d) The finite-difference-method radial orbitals generated by GRASP resemble hydrogenic orbitals like this cut-away of a d orbital, and are useful in complex many-electron systems. All these methods are valuable, but it is often unclear as to which approach can make a complex problem tractable.

Table 1
Convergence of the diagram lines. The lower energy appears 'fully converged' according to the energy eigenvalues, while the last shift of the $2p_{3/2}$ transition only shifts by 0.04 eV. This new approach gives excellent agreement with experiment. The experimental reconstruction is obtained from procedures on experimental data defined in the text. See text for details of CSF basis set generation.

CSF Basis	No. of CSFs	$1s^{-1} \to 2p_{1/2}^{-1}$	$1s^{-1} \to 2p_{3/2}^{-1}$
Titanium			
Minimal basis	61	4504.19	4510.33
$n = 4$	15007	4504.62	4510.83
$n = 5$	58425	4504.90	4511.02
$n = 6$	130543	4504.90	4510.98
Experiment (reconstructed)		4504.94(2)	4510.94(4)

tinguish states. The mixing coefficients, c_r, are determined by diagonalization of the Dirac Hamiltonian, which occurs simultaneously with the optimization of the radial wavefunctions. Current atomic structure computations investigating possible variation of fundamental constants on astrophysical timescales [18] have understandably used only a single configuration with a many-body perturbation theory correction.

A reference CSF set serves as a zeroth order, minimal element basis set. Higher-order corrections are included by increasing the size of the CSF basis. Convergence can be monitored through systematic enlargement of the basis set. The contributions of Auger shifts [19,20] are significant. The CSF basis was created by allowing single and double excitations from the 3d and 4s shell to an active set of virtual orbitals. Virtual orbitals were optimized independently for each angular momentum + parity symmetry. Because the energy ordering of the 3d and 4s subshells differs depending on the core electron configuration, care was taken to exclude CSFs which appeared to be excitations but that actually had a lower energy configuration. Early tests indicated negligible contributions from core-valance excitations which were subsequently excluded from final calculations in order to improve wavefunction convergence.

QED effects (vacuum polarization and self-energy) and finite nuclear mass effects (normal and specific mass shifts) are included perturbatively. Specific mass shifts contribute less than 0.01 eV to transition energies. Our calculation of hydrogenic self-energy screening uses an effective charge model. The screening for upper and lower states in titanium are 0.63 eV and 0.44 eV respectively. Hence the differential screening contribution to transition energies is only 0.19 eV and even a significant uncertainty in screening has no impact on our error budget or conclusions. In any case, these QED uncertainties merely shift the position of the spectrum in energy and do not affect the profile shape which is the central subject of this article.

We used the latest GRASP2K approach [21] to generate electron wavefunctions. This makes use of the bi-orthogonalization procedure of Malmqvist [22] — a transformation of basis states which allows initial and final states to be optimized independently, thus permitting orbital relaxation to be fully taken into account.

In the case of core-ionized titanium, CSFs are so strongly mixed that the single particle approximation is virtually meaningless — only the total atomic angular momentum J is a good quantum number. Recent work has produced results for copper with an accuracy of 0.1 eV [23], however copper is structurally one of the simplest transition metals with a full 3d shell and a single unpaired 4s electron. The most accurate previous MCDF studies of titanium [24,4,25,26] have predicted $K\alpha$ energies to within a few eV, but calculation of the satellite lines which give the spectrum structure is a much more difficult problem. The convergence of the calculated diagram lines for titanium is presented in Table 1 and illustrated in Fig. 2. The lines appear well converged, with oscillations of less than 0.05 eV upon addition of the $n = 6$ virtual orbital layer. Uncertainties inherent in the MCDF method (see for example [27]) do not affect the relative position of diagram and satellite lines, allowing us to obtain a highly accurate analysis of the experimental spectrum.

The titanium $K\alpha$ experimental data was kindly provided by J. Kawai [28]. Measurements were made using a high resolution double-crystal X-ray fluorescence spectrometer and the sample was excited using a Cr anode X-ray tube [29]. As the experimental data was provided without energies, we scaled the peaks to match the experimental results of Anagnostopoulos [30]. Since the experimental resolutions are similar any experiment-dependent peak-broadening shifts will be minor [31].

The result of an MCDF calculation is a 'stick diagram' — a number of lines with a calculated energy and transition strength but no width. To represent a transition we must convolute each line with a Lorentzian and then fit the atomic spectra. The widths of the $K\alpha_1$ and $K\alpha_2$ diagram lines were fitted independently, with all the multiplet lines in each respective peak having the same width (representing a hole-dominated decay broadening). The probabilities of spectator ionization were left as a free parameter, so the width of spectator lines was constrained by a single parameter describing the difference in width between diagram lines and spectator lines.

The resultant fitting parameters are presented in Table 2. There are no fitting coefficients for the relative intensity of the two components of the spectrum, whether for diagram lines or for any particular spectator contributions — *unlike earlier work*, results are fixed by the high-energy, impulse model. Instead, there are fitting coefficients for the relative magnitude of each particular spectator satellite series compared to the diagram lines. Even including the $3d^2$ spectator holes, these are robust and well-defined. The width parameters are generally robust and physical, although the last-added width in a series tends to be broadened, slightly unrealistically, probably to account for minor noise or defects in experimental data or reconstructions. Integrated intensities are derived parameters. The final fit has a χ_r^2 value of 1.17, in excellent agreement with experiment. The excellence of the fit can be seen in Fig. 3; residuals are well contained within 2σ limits and there does
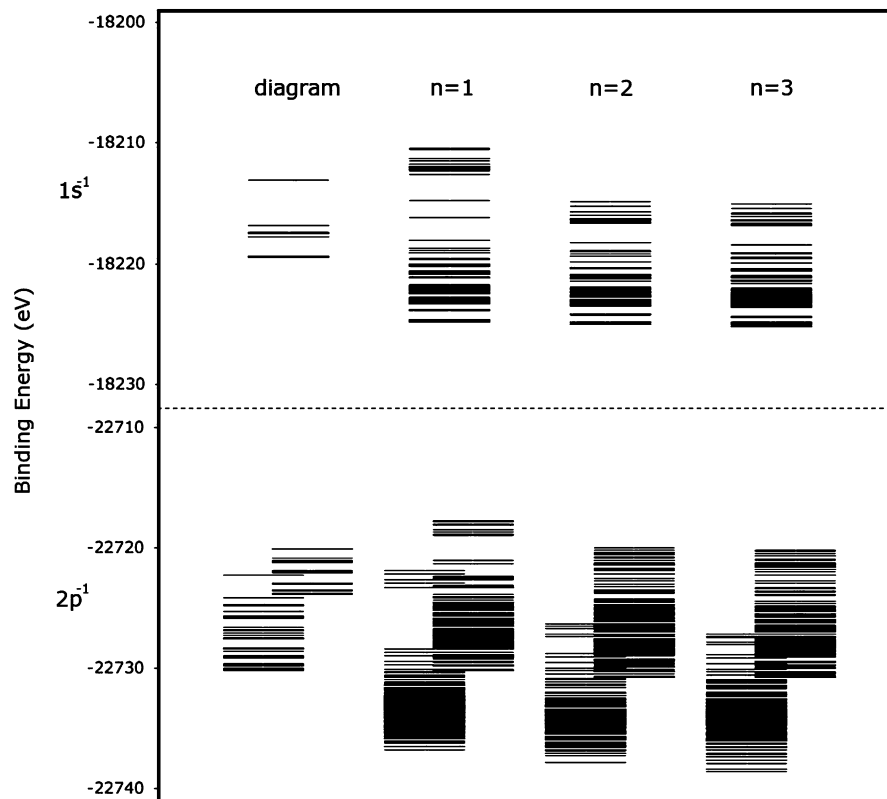
Fig. 2. CSF basis energy levels for computation of the diagram line transitions in titanium, following Table 1. Over a hundred thousand independent eigenstates are coupled in the computation as the basis is expanded towards convergence. Upper energy states have a vacancy in the $1s$ shell and lower energy states have a vacancy in $2p_{1/2}$ (right) or $2p_{3/2}$ (left). Even the complex structure pictured here represents only a small fraction of the total number of interacting energy levels.

Table 2
Fitting parameters for component amplitudes and relative convolved widths for transitions with spectator vacancies in the $3p$ and $3d$ shells compared with the diagram lines. (a) diagram lines only, (b) diagram $+ 3p^{-1}$, (c) diagram $+ 3d^{-1}$, (d) diagram $+ 3p^{-1}, 3d^{-1}$, (e) diagram $+ 3p^{-1}, 3d^{-1}, 3d^{-2}$. The best fit spectrum is plotted in Figs. 3 and 4. Model (e) is clearly required and the sensitivity of the experimental data to the theoretical satellite components is remarkable.

|	Model (a)	Model (b)	Model (c)	Model (d)	Model (e)
Integrated intensity (*relative to total*)					
$K\alpha_1$	0.638(14)	0.621(14)	0.444(14)	0.442(14)	0.453(25)
$K\alpha_2$	0.356(06)	0.345(06)	0.248(08)	0.247(08)	0.253(14)
$3p^{-1}$		0.032(04)		0.015(04)	0.033(05)
$3d^{-1}$			0.351(30)	0.323(32)	0.199(26)
$3d^{-2}$					0.076(18)
Peak intensity (*relative to diagram*)					
$3p^{-1}$		0.030(04)		0.020(08)	0.031(05)
$3d^{-1}$			0.187(16)	0.192(18)	0.154(20)
$3d^{-2}$					0.043(10)
Width (eV)					
Diagram					
$K\alpha_1$	1.76(02)	1.65(02)	1.20(02)	1.20(02)	1.23(03)
$K\alpha_2$	2.35(04)	2.31(04)	1.69(04)	1.71(04)	1.75(04)
$3p^{-1}$					
$K\alpha_1$		1.11(24)		0.67(24)	1.23(25)
$K\alpha_2$		1.77(26)		1.16(26)	1.75(26)
$3d^{-1}$					
$K\alpha_1$			5.12(42)	4.43(42)	3.12(33)
$K\alpha_2$			5.61(44)	4.94(44)	3.64(34)
$3d^{-2}$					
$K\alpha_1$					4.91(90)
$K\alpha_2$					5.43(91)
Peak Separation (eV)					
	6.089	6.117	6.113	6.113	6.134
Reduced χ^2					
	7.42	5.73	1.99	1.62	1.17
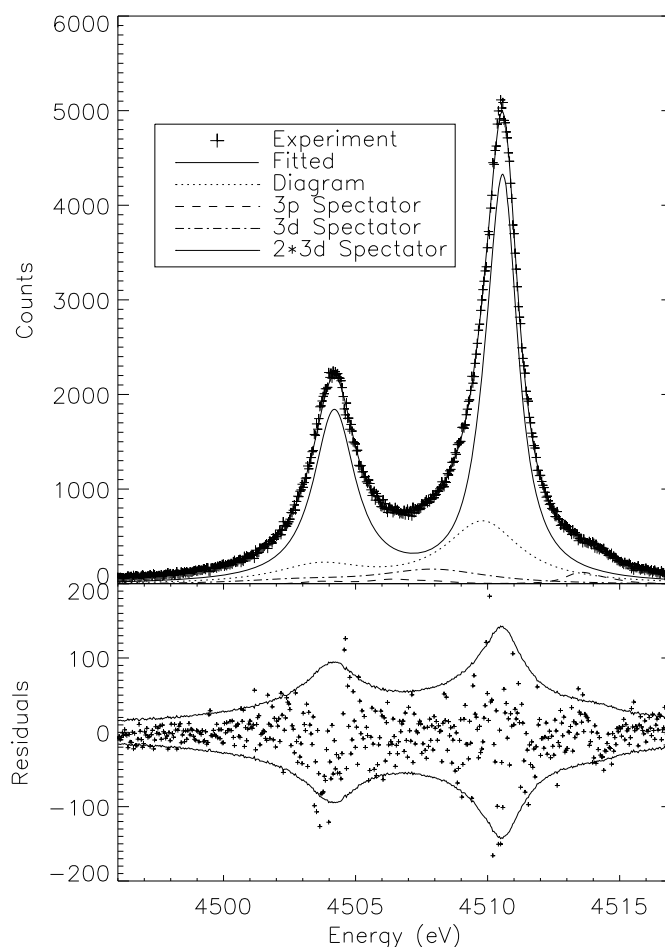
Fig. 3. MCDF calculations fitted to experimental data. The $3d$, $3p$ and $3d^2$ spectator holes all make significant contributions to the profile and asymmetry and are necessary inclusions for *accurate theoretical results*. The solid line in the residual plot represents $\pm 2\sigma$. A detailed look at the spectator contributions is provided in Fig. 4. The relative intensity of each transition within a spectator transitional array is fixed − only the probability of a spectator being present is used in the fit.

Table 3

Comparison of present results with previous work. DF = Dirac Fock, MCDF = Multi-configuration Dirac Fock, RMBT = Relativistic many-body perturbation theory. Two methods were used to separate diagram and satellite lines. In reconstruction A, a series of Lorentzians was fitted to the raw data and the smaller components removed from the spectra. In reconstruction B the satellite components were removed based on MCDF calculations. The two methods produce almost identical results.

Author	Description	$K\alpha_1$	$K\alpha_2$
Mukoyama (1999) [24]	DF	4511.68	4505.16
Deslattes (2003) [4]	DF + RMBT	4510.38(42)	4504.07(44)
Oura (2002) [25]	MCDF	4508.87	4502.66
Shigeoka (2005) [26]	DF	4513.7	4507.8
This work	MCDF	4510.98	4504.90
Experimental (reconstruction A)		4510.94(4)	4504.94(2)
Experimental (reconstruction B)		4510.94(2)	4504.94(2)
Experimental (raw) [30]		4510.90(1)	4504.94(1)

not appear to be any residual structure. A detailed diagram of the titanium satellite structure is given in Fig. 4.

Table 3 compares these results for titanium with those of previous authors. Several authors have calculated energies for the $K\alpha$ doublet but none have considered the satellites, satellite convergence or high-n convergence. No previous calculations are in agreement with experiment. The results presented in this Letter, by contrast, demonstrate excellent agreement for both diagram lines and for the full experimental profile. Previous calculations have used Dirac-Fock or many-body techniques; however ours is the

first to use the bi-orthogonalization procedure and the first to consider full coupling of the core vacancy with the valence electrons.

Spectator intensities, which were a free parameter in our fit, might appear high compared to some earlier theoretical work. Mukoyama [32] and Kochur [13] make *ab initio* determinations for the $3d$ shell shake-off probability of 7.3% and 8.6% respectively for titanium, compared with the fitted value of 28% found herein. However, Anagnostopoulos' results for scandium [33] and both Deutsch's [12] and Chantler's [23] for copper also find spectator populations far higher than predicted by these particular theoretical computations.

The work presented herein has shown that even in these complex, highly excited atoms, a detailed and rigorous approach using modern computational methods can yield absolute transition energies in good agreement with experiment. These results have enabled accurate determination of satellite contributions which for the first time can completely account for the structure of the $K\alpha$ spectrum to within the current limit of experimental accuracy. With these new approaches and methodology, theoretical problems which have resisted earlier understanding can now be investigated thoroughly, especially for complex atoms and inner-shell processes in atomic physics, X-ray optics, plasma science and astrophysics. In particular, dramatic advances over current computations for temporal variation of fundamental constants are possible with a multi-configuration approach that can converge in complex transition metal applications as demonstrated here.
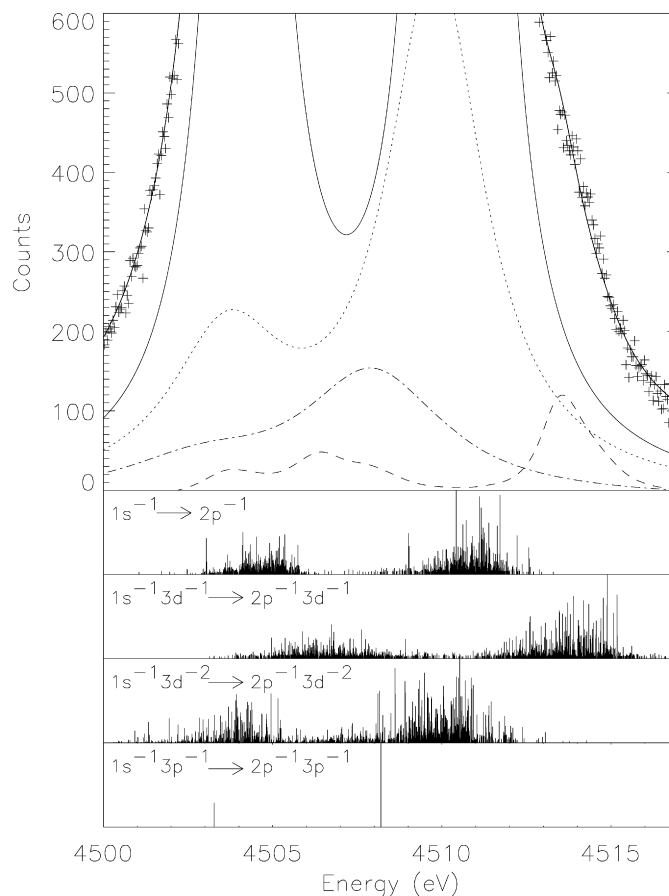
Fig. 4. Large titanium $K\alpha$ spectator contributions predicted and observed. See Fig. 3 for legend. The 'stick figures' below the main picture present the detailed transitions contributing to the spectra. The height of the stick is proportional to the transition strength. These stick figures represent the data prior to correcting for divergence. Prior to fitting we take a weighted average of each $J\Pi$ symmetry.

References

[1] M.T. Murphy, V.V. Flambaum, S. Muller, C. Henkel, Science 320 (2008) 1611.
[2] A.L. Kritcher, P. Neumayer, J. Castor, T. Döppner, R.W. Falcone, O.L. Landen, H.J. Lee, R.W. Lee, E.C. Morse, A. Ng, S. Pollaine, D. Price, S.H. Glenzer, Science 322 (2008) 69.
[3] R.P. Drake, Nature Physics 5 (2009) 786.
[4] R.D. Deslattes, J.E.G. Kessler, P. Indelicato, L. de Billy, E. Lindroth, J. Anton, Rev. Mod. Phys. 75 (2003) 35.
[5] I. Lindgren, S. Salomonson, D. Hedendahl, Phys. Rev. A 73 (2006) 062502.
[6] M. Chen, K. Cheng, W. Johnson, Phys. Rev. A 64 (2001) 042507.
[7] S. Hasegawa, E. Recami, F. Yoshida, L. Matsuoka, F. Koike, S. Fritzshe, S. Obara, Y. Azuma, T. Nagata, Phys. Rev. Lett. 97 (2006) 023001.
[8] K. Nandra, Mon. Not. Roy. Astron. Soc. Lett. 368 (2006) L62.
[9] S. Hansen, A.Y. Faenov, T.A. Pikuz, K. Fournier, R. Shepherd, H. Chen, K. Widmann, S.C. Wilks, Y. Ping, H.K. Chung, A. Niles, J.R. Hunter, G. Dyer, T. Ditmire, Phys. Rev. E 72 (2005) 036408.
[10] J. Kawai, C. Satoko, K. Fujisawa, Y. Gohshi, Phys. Rev. Lett. 57 (1986) 988.
[11] J. Finster, G. Leonhardt, A. Meisel, J. Phys. (Paris) Colloq. 32 (1971) C4-218.
[12] M. Deutsch, G. Hölzer, J. Härtwig, J. Wolf, M. Fritsch, E. Förster, Phys. Rev. A 51 (1995) 283.
[13] A. Kochur, A. Dudenko, D. Petrini, J. Phys. B At. Mol. Opt. 35 (2002) 395.
[14] S. Doniach, M. Sunjic, J. Phys. C Solid State Phys. 3 (1970) 285.
[15] L. Paratt, Phys. Rev. 49 (1936) 502.
[16] M. Deutsch, O. Gang, K. Hämäläinen, C.C. Kao, Phys. Rev. Lett. 76 (1996) 2424.
[17] I.P. Grant, Relativistic Quantum Theory of Atoms and Molecules: Theory and Computation, Springer, 2006.
[18] V.A. Dzuba, V.V. Flambaum, M.G. Kozlov, M. Marchenko, Phys. Rev. A 66 (2002) 022501.
[19] P. Indelicato, S. Boucard, E. Lindroth, Eur. Phys. J. D 3 (1998) 29.
[20] P. Indelicato, O. Gorveix, J.P. Desclaux, J. Phys. B At. Mol. Opt. 20 (1987) 651.
[21] P. Jönsson, X. He, C.F. Fischer, I.P. Grant, Comput. Phys. Commun. 177 (2007) 597.
[22] A. Malmqvist, Int. J. Quantum Chem. 30 (1986) 479.
[23] C.T. Chantler, A.C.L. Hayward, I.P. Grant, Phys. Rev. Lett. 103 (2009) 123002.
[24] T. Mukoyama, B. Song, K. Taniguchi, X-Ray Spectrometry 28 (1999) 99.
[25] M. Oura, H. Yamaoka, K. Kawatsura, K. Takahiro, N. Takeshima, Y. Zou, R. Hutton, S. Ito, Y. Awaya, M. Terasawa, T. Sekioka, T. Mukoyama, J. Phys. B At. Mol. Opt. 35 (2002) 3847.
[26] N. Shigeoka, H. Oohashi, T. Tochio, Y. Ito, T. Mukoyama, A.M. Vlaicu, H. Yoshikawa, S. Fukushima, Phys. Scripta T 115 (2005) 1080.
[27] C.F. Fischer, J. Phys. B At. Mol. Opt. 43 (2010) 074020.
[28] J. Kawai, Personal communication, 2007.
[29] J. Kawai, T. Konishi, A. Shimohara, Y. Gohshi, Spectrochim. Acta B 49 (1994) 725.
[30] D.F. Anagnostopoulos, D. Gotta, P. Indelicato, L.M. Simons, Phys. Rev. Lett. 91 (2003) 240801.
[31] C.T. Chantler, M.N. Kinnane, C.H. Su, J.A. Kimpton, Phys. Rev. A 73 (2006) 012508.
[32] T. Mukoyama, K. Taniguchi, Phys. Rev. A 36 (1987) 693.
[33] D.F. Anagnostopoulos, R. Sharon, D. Gotta, M. Deutsch, Phys. Rev. A 60 (1999) 2018.